Topology of the Υ-decay

PLUTO Collaboration

Ch. Berger, W. Lackas, F. Raupach
I. Physikalisches Institut der RWTH, D-5100 Aachen[1], Federal Republic of Germany

G. Alexander[2], J. Bürger, L. Criegee, H. C. Dehne, R. Devenish[3], G. Flügge[4], G. Franke, Ch. Gerke, G. Knies, E. Lehmann, B. Stella[5], U. Timm, W. Wagner, P. Waloschek, G. G. Winter, W. Zimmermann
Deutsches Elektronensynchrotron, DESY, D-2000 Hamburg, Federal Republic of Germany

O. Achterberg, V. Blobel, L. Boesten, H. Kapitza, B. Koppitz, W. Lührsen, H. Spitzer, R. van Staa
II. Institut für Experimentalphysik der Universität, D-2000 Hamburg[1], Federal Republic of Germany

A. Bäcker[6], S. Brandt, K. Derikum, C. Grupen, H. J. Meyer, B. Neumann, G. Zech
Universität – Gesamthochschule, D-5900 Siegen[1], Federal Republic of Germany

H. J. Daum, H. Meyer, O. Meyer, M. Rössler[7], K. Wacker[6]
Universität – Gesamthochschule, D-5600 Wuppertal[1], Federal Republic of Germany

Abstract. Multihadron events resulting from e^+e^- annihilation at the Υ-resonance are analysed with respect to lowest order QCD which predicts a dominant Υ decay into three vector gluons. Smearing effects due to the gluon fragmentation are so large, however, that no clear 3-jet structure or flatness is expected in the hadron final state. Instead, Monte Carlo simulations predict event structures with thrust and triplicity distributions distinctly different from those of two quark-jet and of phase space like decay mechanisms. The data are in perfect agreement with the 3-vector gluon decay as predicted by QCD and exclude dominantly phase space like or 2-quark jet decays. Also, the decay into scalar gluons is excluded by the data. An upper limit for the Υ-decay into one photon and two gluons is obtained.

1. Introduction

The Υ-meson [1] first produced in proton-nucleus collisions and identified by the decay $Υ \to \mu\mu$ was subsequently observed as a narrow resonance [2] ($m_Υ$

$= 9.46$ GeV; $\Gamma_Υ = (40 \pm^{13}_{8})$ keV) in the reaction $e^+e^- \to Υ \to$ hadrons. It is now generally accepted as a $^3S_1$ bound state of the bottom quark b and its antiparticle $\bar{b}$. In lowest order quantum chromodynamics (QCD) such quark-antiquark ($q\bar{q}$) states are predicted to decay [3, 4] into 3 massless vector particles in complete analogy to the decay [5] of orthopositronium (the $^3S_1$ electron-positron bound state) into 3 photons. The Υ is expected to decay preferentially into three gluons

$$Υ \to ggg.$$

But with $\sim 3\%$ probability the decay should yield a photon and two gluons [4a, f, g]

$$Υ \to \gamma gg.$$

Since gluons are confined in the framework of QCD, we can only observe the hadrons from their fragmentation. Provided a gluon has sufficient energy these hadrons are expected to be collimated as jets about the gluon's original direction. At the Υ-mass, however, the jets overlap considerably in space, so that the 3-jet character cannot be directly revealed. We therefore have to use detailed Monte Carlo studies to search for evidence for an underlying 3-gluon decay structure.

The Υ-decay has been studied with either charged particles [6a] or mainly neutral particles [6e] in early analyses using the properties of the sphericity ellipsoid [7]. In the present paper we include both charged and neutral particles into the analysis. We use as topological measures thrust [8a, b], triplicity [8c], the jet

(a)   (b)
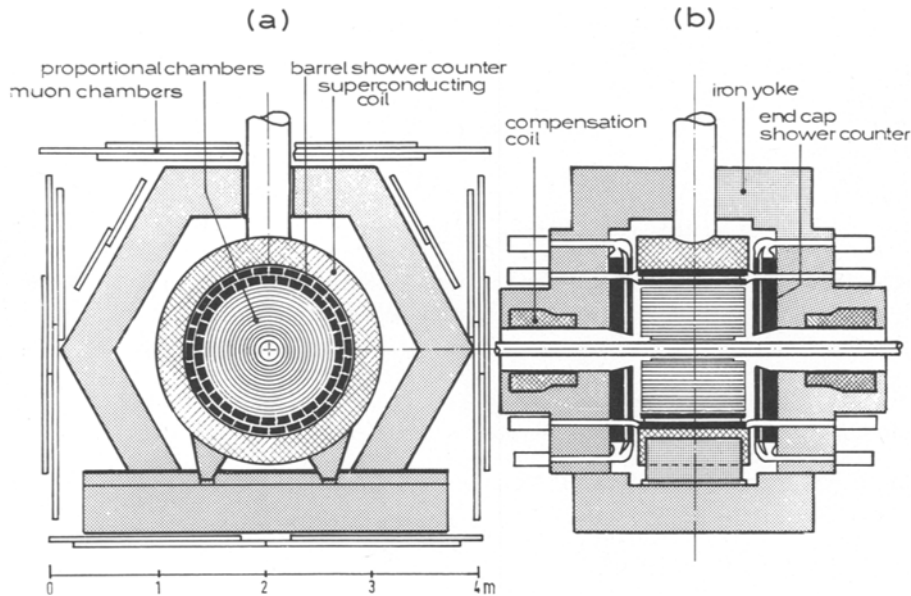

Fig. 1a and b. Experimental set up of the PLUTO detector. Sections **a** perpendicular to and **b** containing the beam axis
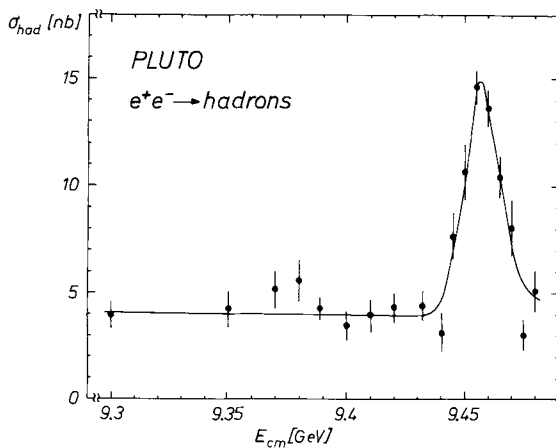

Fig. 2. Hadronic cross section as measured in the Υ region. [The data are corrected except for initial state radiation. The fit to the resonance (solid curve) accounts for radiation and machine resolution]

energies and the angles between jets as constructed by triplicity. We also study the planarity [6a, 6b] of the events.

Although a visual inspection of the decay events does not reveal the three-jet character, the triplicity method is appropriate because it has been shown to be a successful tool at higher energies for analysing the more pronounced three jet character ($q\bar{q}g$) as produced by gluon bremsstrahlung [6c]. First results have already been communicated [9a, 9b]. They show that the inclusion of neutral particles confirms our previous results [6a, 6b].

2. Experimental Procedure

2.1. Experimental Set-Up

The data were obtained with the magnetic detector PLUTO at the DORIS storage rings at DESY. A schematic view of the detector is given in Fig. 1. A superconducting coil producing a magnetic field of 1.69 T contains 10 cylindrical proportional wire chambers for the detection of charged particles and a cylindrical array (barrel) composed of lead-scintillator shower counters (8.6 radiation lengths) and proportional tubes for gamma detection and electron identification. The ends of the cylindrical volume are covered by a second set (endcap) of lead-scintillator shower counters (10.5 radiation lengths) and proportional wire chambers. The shower counters cover 94% of the full solid angle, the cylindrical wire chambers allow momentum measurements of charged particles within 87% of 4π. For muon identification the outside of the flux return yoke is covered with two layers of proportional tubes (65% of 4π).

2.2. Event Selection

For the present analysis events were selected according to the following requirements:

Presence of at least four fully reconstructed charged tracks coming from the interaction vertex.

The reconstructed interaction vertex has a coordinate z which agrees within ± 5 cm with the center of the bunch-bunch collision.
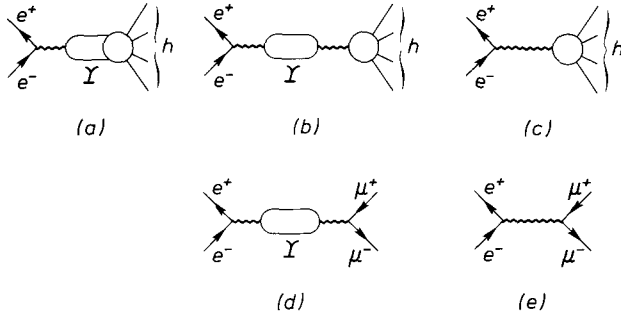
Fig. 3a–e. Processes contributing to hadronic final states in the Υ resonance region **a** from direct decay of the Υ, **b** from Υ vacuum polarization and **c** from the non-resonant continuum. The $\mu^+\mu^-$ final state can be produced from Υ vacuum polarization **d** and from the continuum **e**
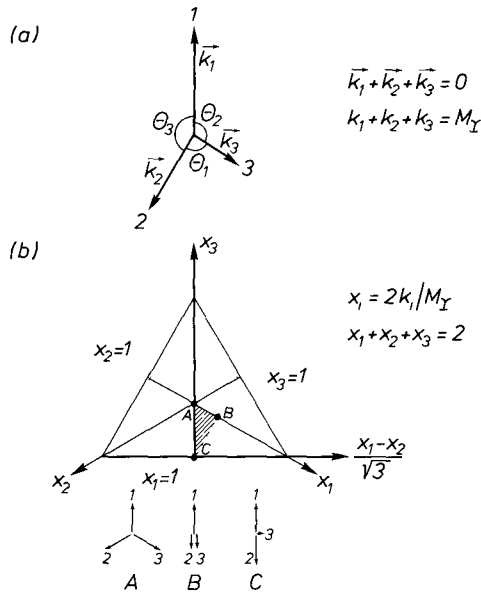

Fig. 4a and b. Quantities used to describe the Υ decay into 3 massless quanta in the Υ rest frame **a** and Dalitz plot of the gluon energies **b**. Momentum conservation limits the population to the dotted triangle. By ordering $x_1 \geqq x_2 \geqq x_3$ this is further restricted to the shaded area

The total observed energy (of charged and neutral particles) is at least 57% of the center of mass energy.

Events with 4 prongs have to be charge balanced. Events with higher multiplicities have to have at least two negatively charged particles.

At least one charged particle must have a z-component of momentum different in sign from those of the others.

We estimate the remaining background from cosmic ray, beam-gas, two-photon and multiprong τ decay events after these cuts to be less than 3%.

2.3. Continuum Subtraction

Data were taken in the energy range $9.25 \text{ GeV} < E_{\text{cm}} < 9.47 \text{ GeV}$. Figure 2 shows the hadronic cross section [10a] obtained for different values of E_{cm} in that range from the numbers of observed events using the monitored luminosity and the acceptance losses computed with the Monte Carlo models of Sect. 3. For our analysis the Υ region was taken to be $9.450 \leqq E_{\text{cm}} \leqq 9.466 \text{ GeV}$. It contains $N_{\text{on}} = 1781$ events. The off-resonance energy region (continuum) was defined by $9.250 \text{ GeV} \leqq E_{\text{cm}} \leqq 9.442 \text{ GeV}$ and contained $N_{\text{off}} = 442$ events.

Hadron events produced at Υ energies originate from three mechanisms: direct Υ decays (Fig. 3a), events from the decay via a virtual photon (vacuum polarisation) (Fig. 3b), and events from the continuum (Fig. 3c). Denoting the corresponding cross-sections with σ_{on} (cross-section in the Υ energy range), σ_{VP} (cross-section for Υ vacuum polarisation), and σ_{off} (cross-section for the non-resonant continuum), the cross section for Υ-production with direct decay is

$$\sigma_{\text{dir}} = \sigma_{\text{on}} - \sigma_{\text{off}} - \sigma_{\text{VP}}.$$

Since for $\mu^+\mu^-$ final states a 'direct' production does not exist (Fig. 3) the third term σ_{VP} can be obtained by scaling the difference for μ-pair production on and off resonance to the hadron production level:

$$\sigma_{\text{VP}} = (\sigma_{\mu\mu}^{\text{on}} - \sigma_{\mu\mu}^{\text{off}}) \cdot \frac{\sigma_{\text{off}}}{\sigma_{\mu\mu}^{\text{off}}}.$$

This gives

$$\sigma_{\text{dir}} = \sigma_{\text{on}} - \sigma_{\text{off}} - \sigma_{\text{off}}(\sigma_{\mu\mu}^{\text{on}} - \sigma_{\mu\mu}^{\text{off}})/\sigma_{\mu\mu}^{\text{off}} = \sigma_{\text{on}} - \sigma_{\text{off}} \cdot \frac{\sigma_{\mu\mu}^{\text{on}}}{\sigma_{\mu\mu}^{\text{off}}}.$$

We use our measured value of

$$\frac{\sigma_{\mu\mu}^{\text{on}}}{\sigma_{\mu\mu}^{\text{off}}} = 1.24 \pm 0.22 \text{ [6a, 11]}.$$

Correcting the above mentioned event rates on and off resonance for the accumulated luminosities the cross-section for direct Υ decays is given by the measured one in the Υ region subtracted by 1.32 times the off-resonance distribution. The subtraction is made bin by bin in all distributions.

3. QCD Predictions on the Parton Level

The QCD predictions are based on the standard matrix element for the decay of the Υ into three vector (1^-) gluons [3, 4]. The 3-body decays of the Υ are completely described in the Υ-rest frame by the momenta $\mathbf{k}_i (i = 1, 2, 3)$ of the 3 quanta. From simple zero mass kinematics one obtains the relation
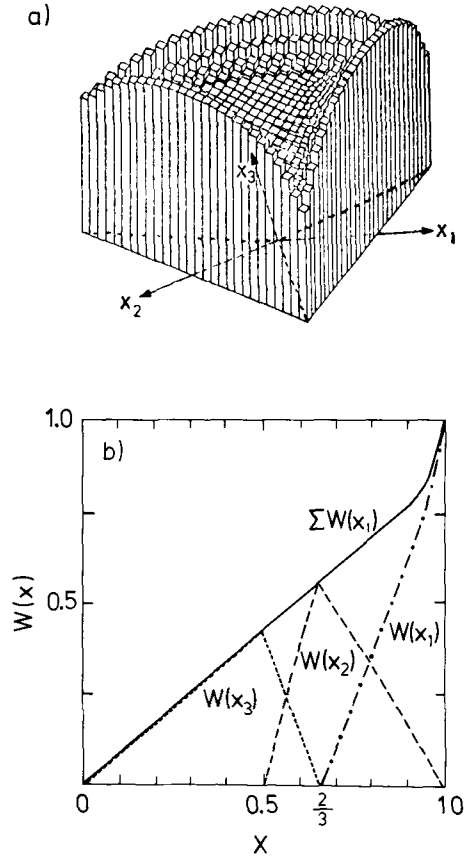
a)

b)

Fig. 5. a Energy Dalitz plots for the Υ-decay into 3 vector gluons (or a photon and 2 vector gluons). The boundaries correspond to the dotted triangle in Fig. 4b. b Energy distribution of the individual gluons in $\Upsilon \rightarrow ggg$ and their sum. (For every event the gluons are ordered such that $x_1 \geqq x_2 \geqq x_3$)

$$x_i = \frac{2 \sin \theta_i}{\displaystyle\sum_{j=1}^{3} \sin \theta_j} \; ; \quad i = 1, 2, 3$$

between the fractional energies $x_i = 2k_i/M_\Upsilon$ of the quanta and the angles θ_i between their directions of flight (see Fig. 4a).

The energies can be used to span a Dalitz plot (Fig. 4b). Its density distribution $W(x_1, x_2, x_3)$ is displayed in Fig. 5a. It is completely symmetric in the three gluon energies [4]. The probability distribution $W(x)$ for a gluon to have an energy x is then obtained by projecting $W(x_1, x_2, x_3)$ onto any of the three axes. Figure 5b shows the relative probability distributions $W(x)$ for the three different gluons as well as their sum. It can already be read from this figure that perfectly pronounced 3-jet events with about equal amounts of energy for each gluon ($x \simeq \frac{2}{3}$) are rare. Many events will have two energetic gluons and one of low energy. At low center of mass energies, where the gluon-jets overlap in space, such a configuration cannot be re-

solved as a 3-jet event. In an alternative but completely equivalent description the three gluon energies can be replaced by the three angles $\theta_i(i = 1, 2, 3)$.

The distribution of the three gluon directions in space is fully determined by theory [4]. For vector gluons QCD predicts [4]

$$W(\cos \theta) \sim 1 + 0.39 \cos^2 \theta,$$

where θ is the angle between the most energetic gluon and the momentum of the electron in the storage ring. Scalar gluons would give rise to a distribution [12a] according to

$$W(\cos \theta) \sim 1 - \cos^2 \theta.$$

The distribution of the angle β between the normal on the three gluon plane and the electron momentum is given by [4]

$$W(\cos \beta) \sim 1 - \tfrac{1}{3} \cos^2 \beta.$$

4. Monte Carlo Programs

For comparison with the data the predictions of the last section are not yet sufficient since we still have to take the gluon fragmentation into account. Lacking an exact theory we use a simple model implemented in a Monte Carlo event generating program (Sect. 4.1 below). Similar programs are used to generate events according to competing models (Sects. 4.2, 4.3). All generated events are passed through a detector simulating program (Sect. 4.4) before being analysed exactly like measured events.

4.1. 3-Jet Generator

The program generates 3 gluon momentum vectors and orients them in space according to Sect. 3. For each gluon a jet with the following properties is generated. The multiplicities of charged and neutral particles are chosen from Poisson distributions with means $\langle n_{ch} \rangle$ and $\langle n_0 \rangle$, respectively which depend on the gluon energy E according to $\langle n_{ch} \rangle = a + b \ln (E/\text{GeV})$ and $\langle n_0 \rangle = c \langle n_{ch} \rangle$. (A logarithmic energy dependence describes the data well in the energy range studied here). The hadrons generated are pions and kaons in the ratio 3:1. Neutral and charged kaons are generated in equal proportion.

The transverse momentum with respect to the gluon direction is chosen according to $f(p_\perp^2) \sim \exp(-p_\perp^2/\langle p_\perp^2 \rangle)$. The longitudinal momenta are selected according to $f(p_\parallel) \sim \exp(p_\parallel/\langle p_\parallel \rangle) + d/p_\parallel$ with a multiplicity dependent cut on $p_\parallel$.

The fragmentation process forms massive jets from mass zero gluons and leads therefore to unavoidable

kinematic distortions. To guarantee nevertheless momentum and energy conservation the generated events are boosted into their rest frame and then all particle momenta are scaled by a common factor.

The free parameters a, b, c, $\langle p_\perp^2 \rangle$, $\langle p_{||} \rangle$, d are ad-adjusted by generating events with only 2 jets at $E_{cm} = 9.4$ GeV and varying the parameters until the properties of the continuum data at 9.4 GeV are reproduced. (For the adjustment of the multiplicity parameters a and b also data at lower energies were used [10c].) This means in essence that the gluon jets are made to fragment very much like the quark jets in the continuum. We want to stress that therefore none of these parameters is obtained from the data. It is also interesting to note that in a 3-jet analysis of our 30 GeV $q\bar{q}g$ data [6d], we get agreement with the measurements if we assume similar properties for the third jet, which is supposed to originate from the gluon, rather than from the quarks.

4.2. 2-Jet Generator

For comparison with the data outside the resonance which show a marked two jet structure we use the model of Field and Feynman [13] as implemented in a program written by Sander [14]. The program generates pairs $Q\bar{Q}$ of a quark and the corresponding antiquark. They are emitted back to back each with half the CM energy and oriented according to a $1 + \cos^2\theta$ distribution with respect to the beam axis. Pairs of $u\bar{u}$, $d\bar{d}$, $s\bar{s}$, and $c\bar{c}$ are generated with relative probabilities $4:1:1:4$. The primary quark (Q) now produces a $q\bar{q}$ pair and forms a meson with the $\bar{q}$, the remaining q forms another $q\bar{q}$ pair etc. The secondary formed pairs $q\bar{q}$ are only allowed to be $u\bar{u}$, $d\bar{d}$ or $s\bar{s}$ pairs. This is motivated by the fact that at this stage $c\bar{c}$ production is highly improbable due to the large mass of the c quark. The details of the transverse and longitudinal momentum distribution in the jets and of the types of mesons formed by the $q\bar{q}$ pairs are fixed by the model [13].

For the 2-jet Monte Carlo events initial state radiation was taken into account by allowing for the radiation of a photon (along the beam direction) with a bremsstrahlung spectrum.

4.3. Phase Space Generators

As a simple alternative to the 3 gluon decay one can also assume the hadronic final state to be given simply by phase space, i.e. a constant matrix element. While phase space is not a realistic model, it stands for reactions which impose no particle correlations except for momentum and energy conservation. Two phase space generators have been used. One (P-PS) generates only

pseudoscalar mesons (pions and kaons in the ratio 3:1). The other (P/V-PS) generates pseudoscalar and vector mesons in equal proportion [15]. The mean multiplicity of the produced particles was chosen such as to reproduce the observed multiplicities.

4.4. Detector Simulation

In order to account properly for detector effects such as finite spatial and energy resolution and limited acceptance all Monte Carlo events are passed through a detector simulation program. It generates proportional chamber and phototube signals corresponding to the trajectories and energies of the particles in the Monte Carlo generated events [10]. The output of this program is passed through the same track recognition, event selection and analysis programs as the real data.

4.5. Angular Distributions

Experimentally, the structure of most angular distributions is not very pronounced, so that we cannot perform significant tests on them within our limited statistics. For example, the distribution of the normal on the three gluon plane carries information on the spin parity assignment of the gluons. Although Monte Carlo calculations have shown that there is a correlation between the 3 gluon input plane and the reconstructed plane [16], this correlation is not sufficiently strong to conclusively test the spin and the parity of the gluons in this fashion with the present statistics.

In contrast, it has been demonstrated [16] that the fastest gluon jet ($\equiv$ the jet with the largest x-value) can be reliably reconstructed by the triplicity method. The experimentally determined thrust axis is closely correlated with the direction of the most energetic gluon. Therefore, the angular distribution of the thrust axis can be compared with expectations for the gluon angular distribution.

5. Topological Tests

In this chapter we want to discuss the various topological quantities, such as thrust, triplicity and planarity. Using Monte Carlo simulations at 9.4 GeV and 30 GeV we study the event reconstruction capability of triplicity and planarity. This includes mainly the correlations between generated event planes, gluon directions or energies, and the corresponding reconstructed quantities.

5.1. Thrust

Because sphericity [7] involves the sum of squares of momenta it has proven to be impossible to calculate

it in the framework of QCD. This had led to alternative measures of "jetness" being proposed that are linear in momentum. We use the thrust variable [4g, 8a, 8b]. Thrust is defined by

$$T = 2 \max \left(\sum_i \tilde{\mathbf{p}}_i'' \right) / \sum_i |\mathbf{p}_i|$$

where the sum $\overset{\sim}{\sum}$ runs over one hemisphere only. $\mathbf{p}_i''$ is the component of $\mathbf{p}_i$ parallel to an axis through the common event vertex and the event is divided into hemispheres by the plane normal to this axis through the vertex. In an event in which there is missing momentum the above definition is somewhat impractical. To overcome this difficulty we use instead

$$T = \max \left(\sum_i |\mathbf{p}_i''| \right) / \sum_i |\mathbf{p}_i|$$

where the sums now run over all particles. The two definitions are identical if all particles in an event are detected without measurement errors.

In an equivalent way thrust can also be defined by partition of momenta into two classes [8a, 8c]

$$T = \frac{1}{\sum\limits_{i=1}^{N} |\mathbf{p}_i|} \max_{C_1, C_2} \left\{ |\mathbf{P}(C_1)| + |\mathbf{P}(C_2)| \right\},$$

where the final state particles with momenta $\mathbf{p}_1, \mathbf{p}_2, \ldots, \mathbf{p}_N$ are grouped into two non-empty classes C_1, C_2 with the total momenta $\mathbf{P}(C_l) = \sum\limits_{i \in C_l} {}_i$, $l = 1, 2$.

This definition has the advantage that it can easily be generalized to n-jet events. For a perfect isotropic event one obtains for thrust $T = \frac{1}{2}$, while a perfect 2-jet event gives $T = 1$.

5.2. Triplicity

To search for a three jet structure the triplicity method [8c] was used. As a natural extension of thrust, triplicity is defined by

$$T_3 = \frac{1}{\sum\limits_{i=1}^{N} |\mathbf{p}_i|} \max_{C_1, C_2, C_3} \left\{ |\mathbf{P}(C_1)| + |\mathbf{P}(C_2)| + |\mathbf{P}(C_3)| \right\},$$

where the final state particles are now grouped into 3 non-empty classes with total momenta $\mathbf{P}(C_l)$, $l = 1, 2, 3$. The values of triplicity vary between $T_3 = 1$ for a perfect 3-jet event and $T_3 = 3\sqrt{3}/8 = 0.65$ for a completely spherical event.

If the momenta of all final state particles were perfectly measured, coplanarity of the 3 jets reconstructed by triplicity would be automatically assured. In the presence of measurement errors and acceptance

losses we enforce coplanarity by adding 1/3 of the missing momentum vector to each of the three jet momenta.

Identifying the coplanar jet directions found in this way with those of the original quanta is only justified if the jets do not significantly overlap in space. Since they actually do overlap at Υ energies, we studied the resolving power of the triplicity method for the Υ-energy and for 30 GeV (in the once expected mass region of a possible $t\bar{t}$ state) using Monte Carlo events. The recovery of the original gluons by the three jets from 3 gluon Monte Carlo events can be characterized by the angles δ_1, δ_2, δ_3 between the directions of the original gluons and the measured triplicity axes both ordered according to their energies.

At the Υ mass the results for the average values of δ_i are (the corresponding values for $E_{cm} = 30$ GeV are given in brackets): $\langle |\cos \delta_1| \rangle = 0.78$ (0.92); $\langle |\cos \delta_2| \rangle = 0.71$ (0.81); $\langle |\cos \delta_3| \rangle = 0.53$ (0.69). In the absence of any correlation we get $\langle |\cos \delta_i| \rangle = 0.50$ ($i = 1, 2, 3$).

This means that we can only reliably reconstruct the two fastest jets at the Υ-mass while the identification of the least energetic jet is marginal.

We have also looked into the reconstruction power of the triplicity method for the gluon energies [16]. Monte Carlo studies show that at the Υ-energy there is a pronounced correlation between the energy of the fastest gluon and the fastest triplicity jet (x_1). The correlation becomes weaker for the gluons with fractional energies x_2 and x_3 [16].

To reconstruct the generated gluon plane using the triplicity method we take the plane spanned by the axes of the two fastest triplicity jets. The average angle α between the normals of the original and reconstructed plane is $\langle |\alpha| \rangle = 43°$ at the Υ-mass. In the absence of any correlations one would naively expect $\langle |\alpha| \rangle = 45°$. However, since the axis of the fastest triplicity jet is used for the plane determination, a small error in the determination of this axis suppresses angles around $0°$. The average "no-correlation" angle turns thus out to be $\langle |\alpha| \rangle = 49°$. It is interesting to note that the average correlation angle at $E_{cm} = 30$ GeV decreases to $24°$.

These investigations show that the direct 3-jet identification improves with increasing energy, being feasable at 30 GeV and only marginal – if at all possible – at the Υ mass.

Since by construction $T_3 > T$ a scatter diagram of T_3 versus T has a boundary as indicated in Fig. 6a. In this figure it is also indicated which regions 3-jet, 2-jet, and spherical events will dominantly populate at high energies. To get an impression how this scatter plot actually looks like we present in Fig. 6b and c Monte Carlo results for center of mass energies of 9.4 GeV and 30 GeV respectively. We can see that there is a considerable overlap for the various models ($q\bar{q}$, ggg,
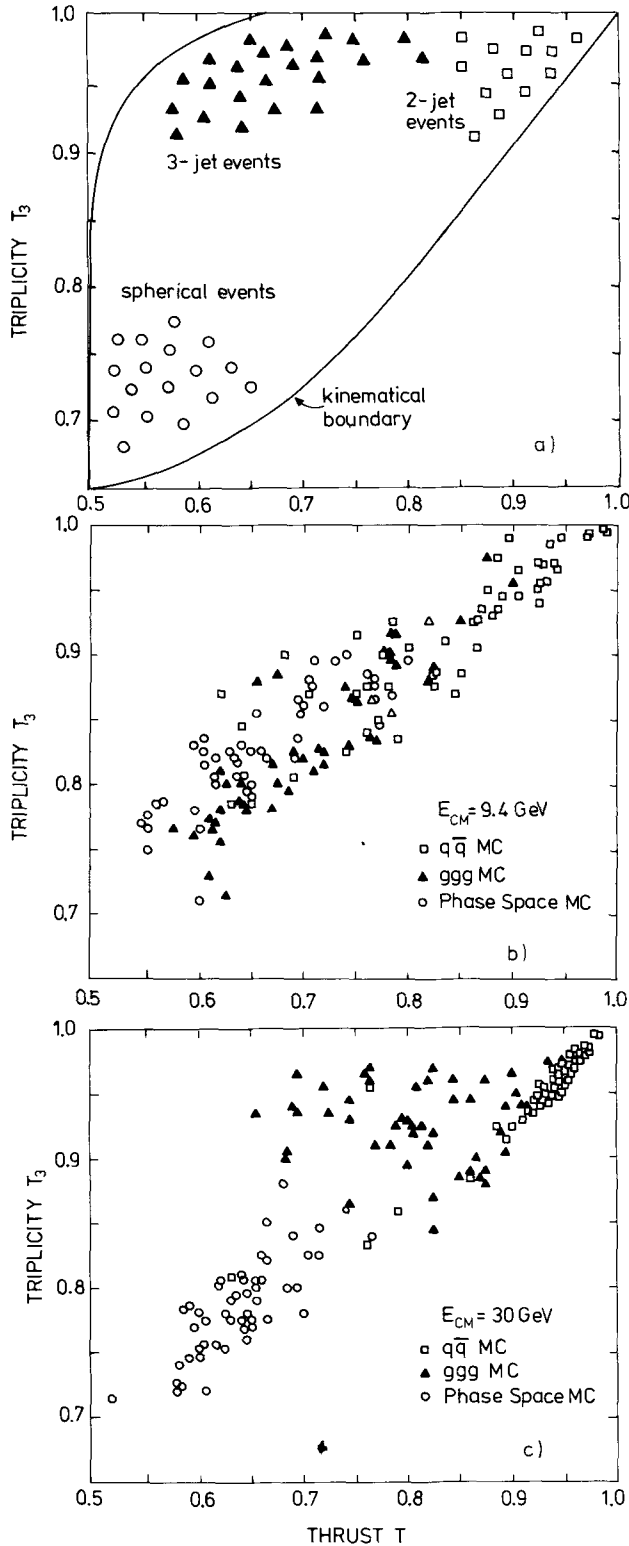
Fig. 6. a Schematic representation of a scatter diagram of triplicity (T_3) versus thrust (T). b,c Scatter diagrams of T_3 versus T for 9.4 GeV and 30 GeV Monte Carlo events for various models ($q\bar{q}$, ggg, PS)

PS) at the Υ-mass while at 30 GeV a separation of the different decay pictures emerges.

5.3. Planarity

An alternative approach to look for the production of three coplanar jets is the planarity method. To this end we calculate the sphericity by forming for each event the sphericity tensor [7]. Ordering the eigenvalues λ_i of that tensor according to $\lambda_1 \geq \lambda_2 \geq \lambda_3$ the sphericity is given by

$$S = 3\lambda_3 \Big/ \left(\sum_{i=1}^{3} \lambda_i \right).$$

A measure of flatness of an event can be extracted from the λ_i according to [6a]

$$Q_i = 1 - \frac{2\lambda_i}{\left(\sum_{i=1}^{3} \lambda_i \right)}.$$

The above ordering of the λ_i implies $Q_1 \leq Q_2 \leq Q_3$. $\frac{Q_1}{Q_2}$ can then be considered as a measure of flatness [6b].

To test the resolving power of the planarity method we can use Monte Carlo events and compare the average angle α between the normals of the original and reconstructed plane. At the Υ-mass we get $\langle |\alpha| \rangle = 42°$, In the absence of any correlations one obtains $\langle |\alpha| \rangle = 49°$. The average correlation angle at $E_{cm} = 30$ GeV is 20°. Also we can compare the direction of the fastest gluon with the direction of the reconstructed Q_3-axis. Denoting this angle by δ we get the Υ-mass $\langle |\cos \delta| \rangle = 0.79$ and $\langle |\cos \delta| \rangle = 0.91$ at $E_{cm} = 30$ GeV. In the absence of any correlations we get $\langle |\cos \delta| \rangle = 0.5$.

These Monte Carlo studies show that the fastest gluon can reliably be reconstructed, but the plane reconstruction power of the planarity method is only marginal at the Υ-mass.

In contrast to triplicitly, planarity is a necessary, but not sufficient condition for a three-jet structure.

In an equivalent way also $\langle p_{out} \rangle / \langle p_{in} \rangle$ can be considered as an indicator for flatness. Here, p_{out} is the momentum out of the triplicity plane and p_{in} the transverse momentum in that plane with respect to the fastest triplicity jet.

6. Analysis of the Υ-data

In this chapter we present the analysis of the Υ-data. We search for an underlying 3-jet structure in the decay events by using the topological quantities thrust, triplicity and planarity. The Υ-data are compared with various theoretical models (3-gluon decay, phase space,
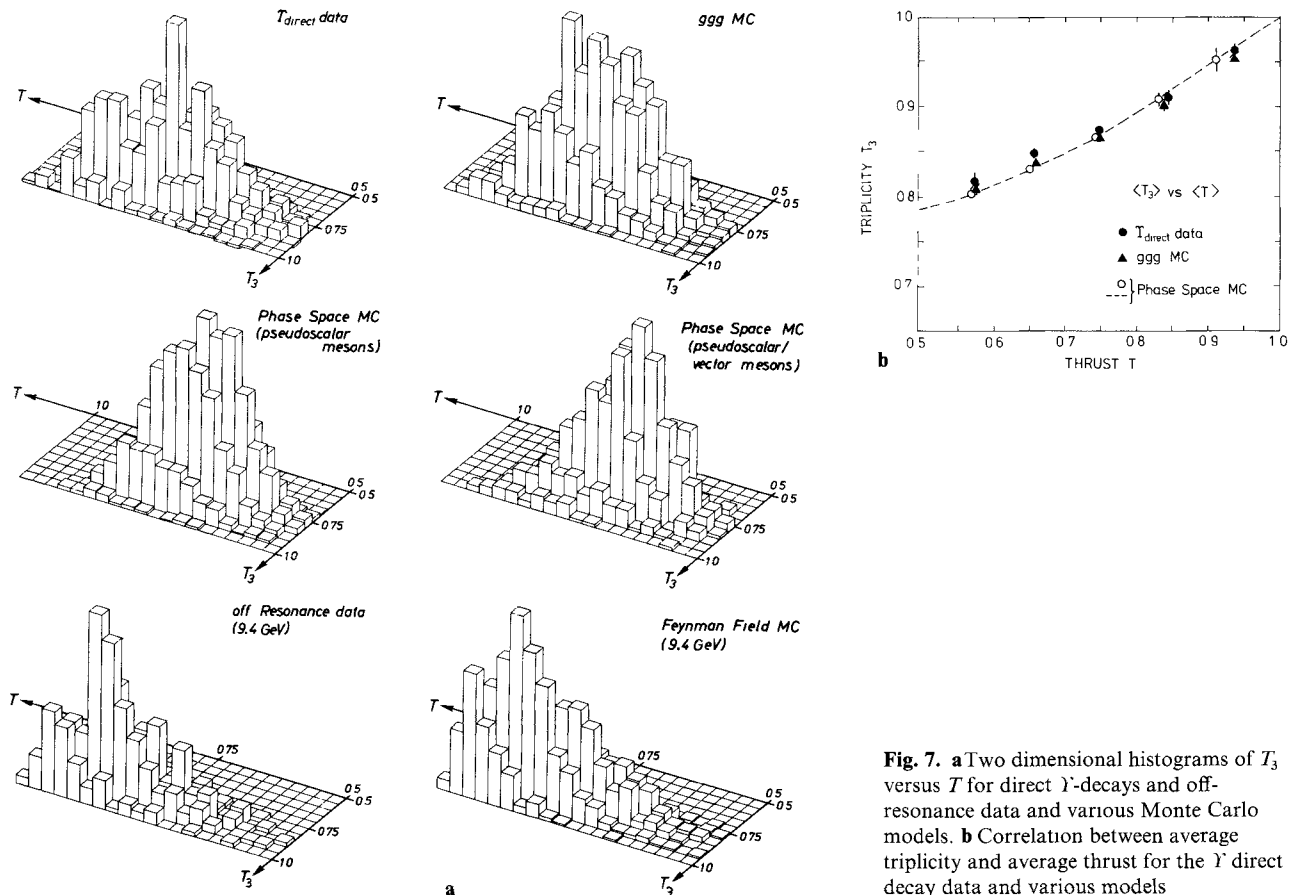
Fig. 7. a Two dimensional histograms of T_3 versus T for direct Υ-decays and off-resonance data and various Monte Carlo models. **b** Correlation between average triplicity and average thrust for the Υ direct decay data and various models

2-jet formation) and off-resonance data. We also briefly discuss competing models (mixed model, scalar gluon model, gluons without color), and compare our measured multiplicities on the Υ and in the nearby continuum with QCD-predictions. For the rare decay mode $\Upsilon \rightarrow \gamma gg$ an upper limit is given.

6.1. Thrust and Triplicity Analysis

In Fig. 7a we present two-dimensional histograms T_3 versus T for Υ-direct data and for the off-resonance data as well as for the 3-jet, 2-jet and phase space Monte Carlo events. The data are uncorrected. Detector effects are taken into account in the Monte Carlo simulation. Although it is difficult to draw firm quantitative conclusions from these two-dimensional histograms one can see that there is a striking similarity between the Υ-direct data and the 3-gluon Monte Carlo, whereas the phase space Monte Carlo, 2-jet Monte Carlo, and off-resonance data look different. Also the off-resonance data agree with the 2-jet picture. The results from the two different phase space Monte Carlos are very similar, but also very different from the 2-jet events.

Thrust and triplicity are strongly correlated. In Fig. 7b we show the dependence of the average triplicity on the average thrust. At thrust values of $T > 0.7$ all models fall on one common curve which also describes the data. Only for the two lowest thrust bins there is a slight indication of the occurrence of 3-jet events since there $\langle T_3 \rangle_\Upsilon > \langle T_3 \rangle_{PS}$ for the same thrust values.

The projections of the two-dimensional histograms (Fig. 7a) onto their axes allow a more quantitative comparison. Because of the correlation between thrust and triplicity we only show here the projection onto the thrust axis (Fig. 8). The tentative conclusions drawn from the two-dimensional histograms are confirmed. The 3-gluon Monte Carlo describes the data best; predominantly 2-jet like models are ruled out. The off-resonance data are very well described by the 2-jet Monte Carlo.

Also phase space is ruled out. First there is a general argument against phase space like topologies at the Υ. Although the average sphericity $\langle S \rangle$ or the average value of $\langle 1 - T \rangle$ of the J/ψ-decay can still be described by phase space [6a, 17], both quantities increase for any phase space model with increasing particle multiplicity. However, on the Υ we find $\langle S \rangle$
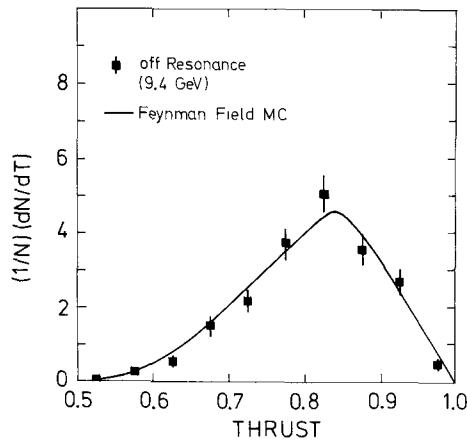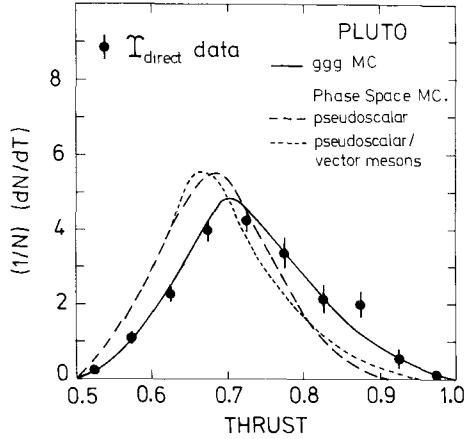
Fig. 9. Thrust distribution for the Υ-direct decay, corrected for detector deficiencies

Fig. 8. Experimental distributions in thrust for Υ-direct (top) and off-resonance events (bottom) compared to various Monte Carlo models
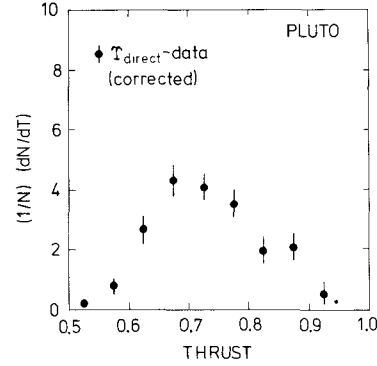
and $\langle 1 - T \rangle$ comparable to the corresponding quantities on the J/ψ, in spite of a factor of two higher multiplicity. As Table 1 shows, the thrust values for the Υ and for phase space Monte Carlos differ by more than 3 standard deviations. This is a strong evidence that the Υ cannot be described by uncorrelated particle emission, like simulated in the phase space model (see also [18]).

A corrected thrust distribution on the Υ is shown in Fig. 9. The correction is done bin by bin, and the correction factor is derived from generated Monte Carlo events in comparison to how these events look like in our detector. From the comparison of Figs. 8 and 9 it can bee seen that the correction factors are quite small. The corrected average thrust on the Υ is $\langle T \rangle = 0.73 \pm 0.01$.

Table 1. Mean values of thrust, triplicity, triplicity related observables (x_i, θ_i) and flatness measures for Υ-direct and off resonance data and various Monte Carlo models. (The errors for data are statistical. For Monte Carlo they contain the systematic uncertainties in the models)

|	Υ-direct data	3 (vector) gluon Monte Carlo	Phase-space Monte Carlo (pseudo-scalar-mesons)	Phase-space Monte Carlo (pseudo-scalar and vector mesons)	3 (scalar) gluon Monte Carlo	Off-resonance data	Field-Feyman Monte Carlo
$\langle T \rangle$	0.732 ± 0.004	0.72 ± 0.01	0.69 ± 0.01	0.69 ± 0.01	0.80 ± 0.01	0.808 ± 0.004	0.80 ± 0.01
$\langle T_3 \rangle$	0.870 ± 0.002	0.86 ± 0.01	0.84 ± 0.01	0.84 ± 0.01	0.90 ± 0.01	0.910 ± 0.002	0.90 ± 0.01
$\langle x_1 \rangle$	0.862 ± 0.003	0.86 ± 0.01	0.83 ± 0.01	0.83 ± 0.01	0.90 ± 0.01	0.909 ± 0.003	0.91 ± 0.01
$\langle x_2 \rangle$	0.715 ± 0.004	0.72 ± 0.01	0.70 ± 0.01	0.71 ± 0.01	0.77 ± 0.01	0.733 ± 0.005	0.75 ± 0.01
$\langle x_3 \rangle$	0.423 ± 0.005	0.42 ± 0.01	0.47 ± 0.01	0.46 ± 0.01	0.33 ± 0.01	0.358 ± 0.007	0.34 ± 0.01
$\langle \theta_1 \rangle$	$82.6° \pm 0.9°$	$83° \pm 1°$	$90° \pm 1°$	$90° \pm 1°$	$68° \pm 1°$	$68.8° \pm 1.1°$	$70° \pm 1°$
$\langle \theta_2 \rangle$	$126.4° \pm 0.6°$	$126° \pm 1°$	$124° \pm 1°$	$124° \pm 1°$	$133° \pm 1°$	$132.8° \pm 0.8°$	$131° \pm 1°$
$\langle \theta_3 \rangle$	$151.0° \pm 0.5°$	$151° \pm 1°$	$146° \pm 1°$	$146° \pm 1°$	$159° \pm 1°$	$158.4° \pm 0.6°$	$159° \pm 1°$
$\langle Q_1/Q_2 \rangle$	0.368 ± 0.009	0.37 ± 0.01	0.40 ± 0.01	0.40 ± 0.01	0.35 ± 0.01	0.327 ± 0.009	0.35 ± 0.01
$\left\langle \frac{\langle p_{out}\rangle}{\langle p_{in}\rangle} \right\rangle$	0.548 ± 0.007	0.55 ± 0.01	0.56 ± 0.01	0.56 ± 0.01	0.52 ± 0.01	0.498 ± 0.008	0.52 ± 0.01
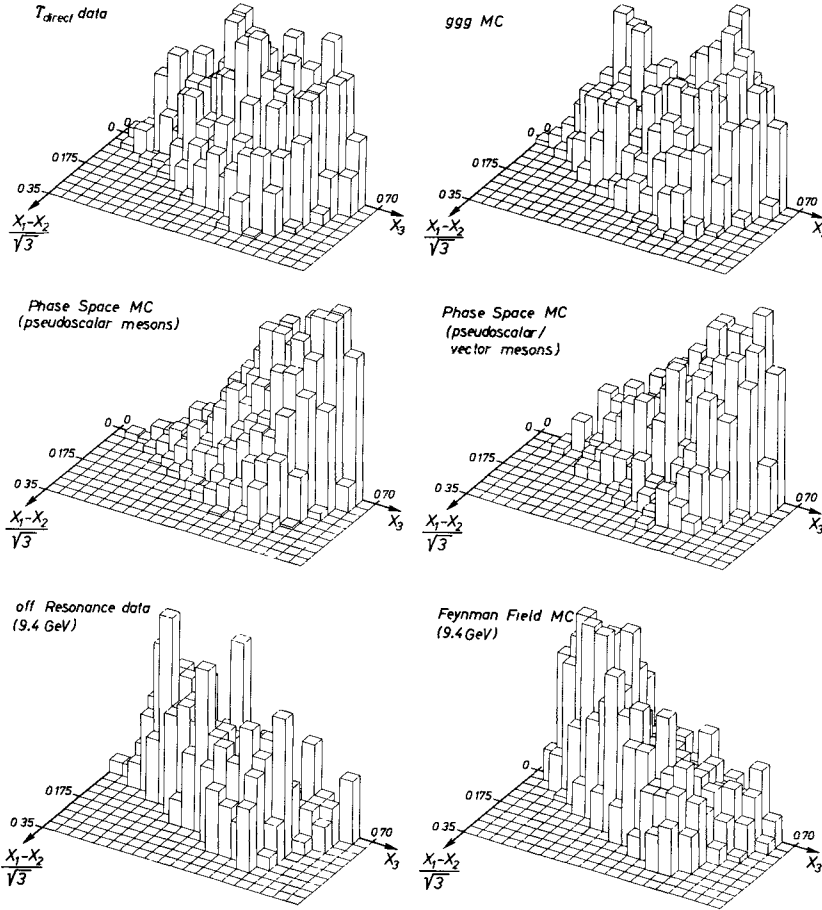
Fig. 10. Two-dimensional histograms representing the 3-jet energy Dalitz plot for Υ-direct and off resonance data and various Monte Carlo models

Instead of using T_3 and T we can present the data also in terms of the fractional energies x_i of the jets as constructed by triplicity. If the three jets were completely separated in space the fractional energies x_i would be essentially independent of the fragmentation of the gluons and would depend only on the matrix element. The topological quantities T and T_3, however, always depend on the details of the gluon fragmentation. Therefore, the x_i-distributions carry additional information. In Fig. 10 we show the two-dimensional histograms representing the 3-jet energy Dalitz plots for Υ-direct and off-resonance data and various Monte Carlo models. Unfortunately, at Υ-energies the constructed jets are too weakly correlated to the gluon energies as to draw firm conclusions to the Υ-decay matrix element from this plot. Only in the limit of high energies the observales x_i agree with the fractional energies of the gluons.

Even though the x_i do not have physical significance in simulated phase space and $q\bar{q}$ events, as discussed above, we show their respective Dalitz plots also to exhibit the topological differences of these events from the Υ direct decay events.

The data and models shown in Fig. 10 can be discussed as follows: The two phase space models are very similar. Keeping in mind that $\sum_i x_i = 2$, one expects in the x_3-variable a clustering of the events near $x_3 = \frac{1}{3}\sum_i x_i$, because phase space will predominantly be interpreted by three jets with approximate equal amounts of energy if the triplicity method is used.

For the off-resonance data, where on the other hand we expect a pronounced 2-jet structure, we indeed find that the region of large x_3 is significantly depleted as compared to the phase space models. This feature is also borne out by the corresponding Monte Carlo simulation of 2-jet events. As far as the Υ-direct data are concerned they fall inbetween the phase space models and the 2-jet model. The energy Dalitz plot is more uniformly distributed and it is also reproduced by the 3-gluon decay picture.

The merits of presenting the results in terms of the x_i variables which are qualitatively different from T and T_3 will become more apparent at higher $q\bar{q}$-resonances.

Figure 11 shows the projection of the two-dimensional histograms on the x_1-axis, which is the distribu-
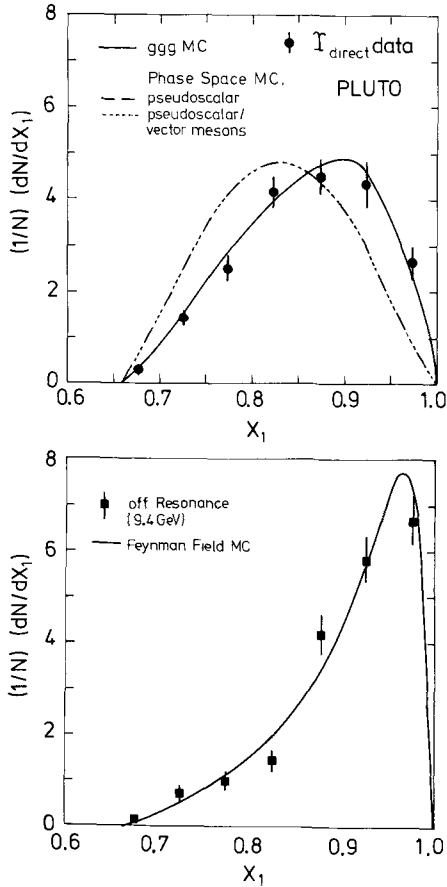
Fig. 11. Experimental distribution of the reconstructed reduced energy x_1 of the fastest triplicity jet for Υ-direct and off-resonance data compared to Monte Carlo calculations for various models
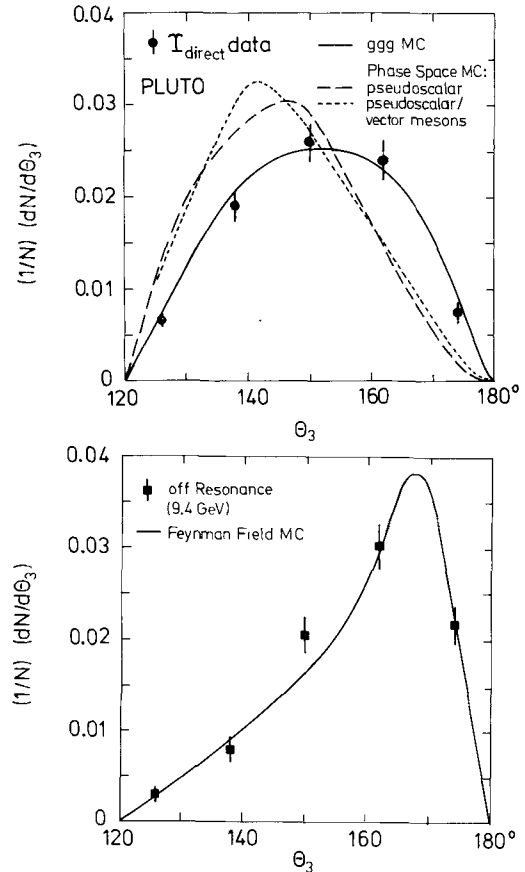

Fig. 12. Experimental distribution of the reconstructed angle θ_3 between the two fastest triplicity jets for Υ-direct and off-resonance data compared to various Monte Carlo models

tion of the most energetic triplicity jet. We have ascertained by Monte Carlo studies [16] that x_1 can be most reliably reconstructed.

In an equivalent way the angles θ_i between the constructed triplicity jets can be used to describe the Υ-data. But since the angles θ_i are directly related to the x_i, the θ_i-plots carry no additional information. Therefore we only show the distribution of the best reconstructed angle θ_3 (Fig. 12). The conclusions drawn above from the T, T_3 plots and its projection on T are confirmed in the x_1 and θ_3 distributions. Further two-dimensional histograms and distributions for other variables are presented in [16].

We have also investigated whether a mixed model (50% phase space plus 50% two-jet) describes our data. The idea of a mixed model was derived within the framework of the quark fusion model [12b]. We compare the thrust and θ_3 distribution with the 3 gluon decay and the mixed model and find that the 3 gluon decay picture of the Υ is slightly favored over such a mixed model (Fig. 13).

As an information additional to the distributions discussed above, the results of this section are summarized in Table 1 in form of mean values for T, T_3, x_i, θ_i for the Υ-direct and off-resonance data, as well as the various Monte Carlo models and an additional scalar gluon model [12c].

The Υ-direct data are very well reproduced by the 3-gluon model, while the other models fail to describe the Υ-data.

6.2. Planarity Analysis

The planarity analysis is done along the lines as described in Sect. 5. We have determined the Q_i-values using the sphericity method. The results are also given in Table 1 in form of the mean values of $\langle Q_1/Q_2 \rangle$ for the different sets of data and models. We have also looked into the results for $\langle\langle p_{\text{out}} \rangle/\langle p_{\text{in}} \rangle\rangle$. They are consistent with the $\langle Q_1/Q_2 \rangle$ values. No significant differences are observed between phase space, Υ-decays, and 3 gluon Monte Carlo events.
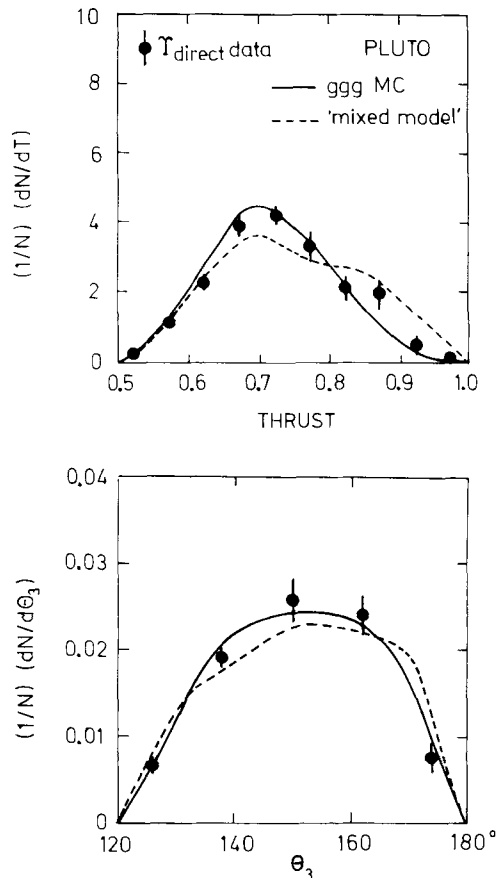
Fig. 13. Thrust and θ_3 distribution of Υ-direct decay events in comparison to a 3 gluon Monte Carlo and a mixed model (50% phase space, 50% $q\bar{q}$)
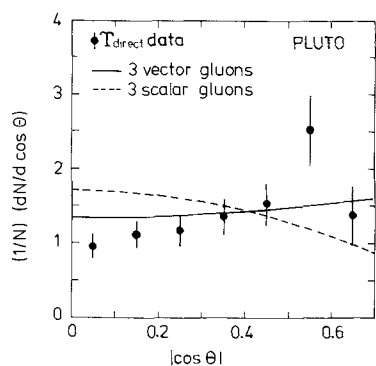

Fig. 14. Corrected experimental distribution of $|\cos \theta|$. θ is the angle between the thrust axis and the beam axis. The curves are predicted for Υ-decay into vector and scalar gluons, respectively

6.3. Discussion of the Triplicity and Planarity Analysis

The methods used for the analysis of the Υ-data give consistent results. We observe a good agreement between QCD predictions and the Υ-direct data. The average quantities shown in Table 1 may indicate that the Υ-decay events are showing some – however marginal – degree of flatness.

Although we are unable to directly resolve the 3-jet structure of the events our data agree in all aspects with the results of the 3-gluon Monte Carlo simulation.

6.4. Vector Gluons and Competing Models

In Sect. 3 we have presented the theoretical predictions for the distribution of the thrust axis. Figure 14 shows our data corrected for fragmentation and detector deficiencies along with the predictions. The data are consistent with vector gluons while they cannot be described by scalar gluons.

The case against scalar gluons becomes even more convincing if we consider the probability distributions $W(x_i)$ as introduced in Sect. 3. Theory [12a] predicts that all events would have one gluon with very low or vanishing energy: the events would appear as two jet events. We have written a Monte Carlo generator for the Υ-decay into scalar gluons, including subsequent fragmentation into jets and passage through the detector. A full triplicity analysis of a sample of such events has been performed [16]. We do not show the distributions here since, of course, they are very similar to those obtained with the 2-jet Monte Carlo program.

This can also be seen from Table 1 which contains a column for the scalar gluon model. Since the predicted values do not at all describe the Υ-direct data the scalar gluon hypothesis is definitely excluded.

Furthermore the assumption of a Υ-decay into pseudoscalar gluons is in severe conflict with the observed level splittings in the charmonium system. Thus, pseudoscalar gluons are also excluded [12a, 12d].

The possibility of vector gluons without color has also been discussed in the literature [12c]. Given colorless gluons the decay $\Upsilon \rightarrow g \rightarrow q\bar{q}$ would be possible in lowest order. Obviously then there would be no difference between the event structure on the Υ-resonance and the continuum. The hypothesis of colorless gluons is therefore in complete contradiction to the data.

6.5. Multiplicity on the Υ

According to the prediction of QCD [4e, 4h, 4a, 4j] the multiplicity of the Υ should be higher compared to the nearby continuum. If the gluon fragments like a single quark one expects from the multiplicity of two jet events at center of mass energies around 6 GeV

$$\langle n_{\mathrm{ch}} \rangle_{\rightarrow ggg} \sim 7\text{--}8.$$

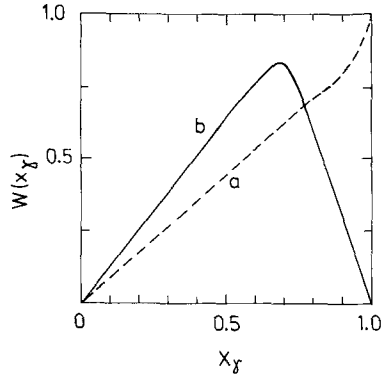**Fig. 15a and b.** Expected photon spectrum of the decay $\Upsilon \to \gamma gg$ **a** for massless gluons (positronium model) **b** with fragmentation of gluons (see text)

But it has been argued that the gluon could fragment with a higher multiplicity, since its average color charge is $\frac{9}{4}$ times larger than that for quarks [4j]. This would lead to

$$\langle n_{\mathrm{ch}} \rangle_{\Upsilon \to ggg} \sim 9.$$

Most theoretical estimates indicate an expected increase of 1.5–3 units in charged multiplicity [4h]. The average charged multiplicity for Υ-direct decays measured in this experiment is

$$\langle n_{\mathrm{ch}} \rangle_{\Upsilon \to ggg} = 8.2 \pm 0.1$$

while for the continuum data we obtained [20]

$$\langle n_{\mathrm{ch}} \rangle_{\mathrm{off-resonance}} = 6.9 \pm 0.1.$$

The multiplicities have been corrected for detector efficiencies and acceptance losses.

Compared to the continuum data we see a clear increase of the charged multiplicity of*

$$\Delta n_{\mathrm{ch}} = 1.3 \pm 0.2.$$

This increase of $\Delta n_{\mathrm{ch}} = 1.3$ at the Υ reflects according to the theoretical considerations of Bigi and Nussinov [4h] a larger dynamical increase of $\Delta n_{\mathrm{ch}} = 2.0$ in 3-gluon jet processes as compared to $q\bar{q}$ jets. Our data on the Υ are thus in good agreement with expectations based on QCD calculations.

6.6. Search for the Υ-Decay into one Photon and two Gluons

In our hadronic event sample we have looked for events with an isolated high energy photon from the

decay $\Upsilon \to \gamma gg$ as suggested in [4f]. We required one photon with a reduced energy $x_\gamma = 2E_\gamma / M_\Upsilon > 0.7$ being the only particle in one of the triplicity jets. To reduce background from beam gas interactions and heavy lepton decays we further required that at least one of the remaining triplicity jets contains more than one charged particle with momentum above 300 MeV/c. We find 12 events of this type on the Υ-resonance.

The background from unresolved π^0 and η has been estimated for the various models discussed above. For the phase space models we find a background of 0 events, for the two-jet model 7 events, and for the 3-gluon model 11 events.

To compute the detection efficiency for the decay $\Upsilon \to \gamma gg$ we have used a Monte Carlo program treating the gluon fragmentation as described in Sect. 4.1. The energy spectrum of Fig. 5b $\left(\sum_{i=1} W(x_i) \right)$ as well known from the positronium decay is drastically affected by the transition of massless gluons into massive jets. The probability of having a photon with $x_\gamma > 0.7$ drops from 50% for the positronium model to 29% for our model (Fig. 15)*. The one obtained excess event (compared to the background calculated on the basis of the 3-gluon model) – taken at face value – would correspond to a branching ratio of $\Gamma(\Upsilon \to \gamma gg)/\Gamma(\Upsilon_{\mathrm{dir}}) = 2.6\%$. Expressed as an upper limit for the Υ-decay into one photon and two gluons we obtain

$$\frac{\Gamma(\Upsilon \to \gamma gg)}{\Gamma(\Upsilon_{\mathrm{dir}})} < 27\%$$

at 90% confidence level. This can be compared to the experimental value of the LENA-Collaboration $(\Gamma(\Upsilon \to \gamma + \mathrm{hadrons})/\Gamma(\Upsilon \to \mathrm{hadrons}) < 5\%$ at 95% confidence level [21] and to the theoretical prediction based on QCD of $\sim 3\%$ [4a, 4f, 4g] if we assume $\Gamma(\Upsilon \to ggg) = \Gamma(\Upsilon_{\mathrm{dir}})$.

7. Conclusions

In a jet analysis of $e^+ e^-$-annihilation in the Υ-region we have established the following facts:

(i) The Υ-decay topology has characteristics very different from those of the continuum. The continuum data are well described by assuming $e^+ e^-$-annihilation into a quark-antiquark pair producing two hadronic jets.

(ii) The two jet character of Υ events is stronger than for phase space and weaker than for off-resonance events.

---

* We only quote the statistical errors of the multiplicities. The systematic uncertainties in the "on" and "off"-resonance multiplicities are expected to cancel out in the difference Δn_{ch}

---

* It is interesting to note that our calculated photon spectrum seems to agree qualitatively with the spectrum observed on the J/ψ at SPEAR [19]

(iii) The rather detailed features of the Υ-direct decay that are visible in the distributions of thrust, triplicity, triplicity related observables (x_i, θ_i) and angular orientation of the events are very well described by the QCD-prediction of Υ-decay into 3 vector gluons with subsequent fragmentation into jets.

(iv) As expected from the width of the fragmentation distributions neither the triplicity nor the planarity analysis gives positive evidence for the production of three jets in the Υ-decay which are separated in space. The correlation between the parton and triplicity or planarity plane is too weak to exploit it with the present statistics for a spin analysis. However, scalar gluons are ruled out on the basis of the thrust axis angular distribution.

(v) The Υ-direct data cannot be described by any one of the two different phase space models used.

(vi) A mixed model (50% phase space, 50% $q\bar{q}$) does not describe the data as well as the 3 gluon decay of the Υ does.

(vii) A competing model of the Υ-decay into 3 scalar gluons, which predicts essentially only two hadronic jets in the final state, is clearly ruled out. The same holds for the assumption of colourless gluons.

(viii) The observed increase in multiplicity on the Υ is consistent with the prediction of QCD.

(ix) As an upper limit for the branching ratio $\Gamma(\Upsilon \to \gamma gg)/\Gamma(\Upsilon \to ggg)$ a value of 27% was obtained.

References

1. S. W. Herb et al.: Phys. Rev. Lett. **39**, 252 (1977)
   W. R. Innes et al.: Phys. Rev. Lett. **39**, 1240 (1977)
2. a) PLUTO Collaboration, Ch. Berger et al.. Phys. Lett. **78** B, 243 (1978)
2. b) PLUTO Collaboration, Ch. Berger et al.: Phys. Lett. **93** B, 497 (1980)
2. c) DASP II Collaboration, C. W. Darden et al.. Phys Lett. **78** B, 246 (1978)
2. d) LENA Collaboration, B. Niczyporuk et al.. DESY 80/53 (1980)
2. e) H. Schröder, DESY 80/61 (1980)
2. f) CLEO-Collaboration, D. Andrews et al.: Phys. Rev Lett. **44**, 1108 (1980)
2. g) CUSB-Collaboration, T. Böhringer et al.: Phys. Rev. Lett. **44**, 1111 (1980)
2. h) CLEO-Collaboration, Contributed paper for the International Conference on High Energy Physics, Madison, July 1980, Report CLNS 80/464 (1980)
2. i) LENA Collaboration, J. K. Bienlein et al.: Phys. Lett. **78** B, 360 (1978)
3. T. Appelquist, H. D. Politzer: Phys. Rev. Lett. **34**, 43 (1975); Phys Rev. D **12**, 1404 (1975)
4. a) K Koller, T. F. Walsh: Phys Lett. **72** B, 227 (1977) [E: **73** B, 504 (1978)]
4. b) K. Koller, T. F. Walsh: Nucl. Phys. B **140**, 449 (1978)
4. c) K. Koller, H. Krasemann, T. F. Walsh: Z. Phys. C.–Particles and Fields **1**, 71 (1979)
4. d) T. A. DeGrand, Y. G. Ng, S. H. H. Tye: Phys. D **16**, 3251 (1977)
4. e) S. J. Brodsky, T. A. DeGrand, R. R. Horgan, D. G. Coyne: Phys Lett. **73** B, 203 (1978)
4. f) H. Fritzsch, K H. Streng: Phys. Lett. **74** B, 90 (1978)
4. g) A. de Rujula, J. Ellis, E. G. Floratos, M. K. Gaillard: Nucl. Phys. B **138**, 387 (1978)
4 h) I. I. Y. Bigi, S. Nussinov: MPI-PAE/PTh 44/78 (1978)
4. j) S. Brodsky, J. Gunion: Phys. Rev. Lett. **37**, 402 (1976)
5. A. Ore, J. L. Powell: Phys. Rev. **75**, 1696 (1949)
6. a) PLUTO Collaboration, Ch. Berger et al.: Phys. Lett. **82** B, 449 (1979)
6. b) G. Knies: Proceedings of the XIVth Rencontre de Moriond, p 99 (1979)
6. c) PLUTO Collaboration, Ch. Berger et al.: Phys. Lett. **86** B, 418 (1979)
6. d) PLUTO Collaboration, Ch. Berger et al.: DESY 80/93 (1980)
6. e) LENA Collaboration, F. H. Heimlich et al.: Phys. Lett. **86** B, 399 (1979)
7. J. D Bjorken, F. J. Brodsky: Phys. Rev. D **1**, 1416 (1970)
8. a) S. Brandt, Ch. Peyrou, R. Sosnowski, A. Wroblewski: Phys. Lett. **12**, 57 (1964)
8. b) E. Fahri: Phys. Lett. **39**, 1587 (1977)
8. c) S. Brandt, H. D. Dahmen: Z. Phys. C – Particles and Fields **1**, 61 (1979)
9. a) PLUTO Collaboration, Ch. Berger et al.: (talk by S. Brandt), Proceedings of the International Conference on High Energy Physics, Geneva 1979, p. 338 (and DESY 79/53)
9. b) PLUTO Collaboration, C. Grupen: Talk presented at the XX Int. Conf. on High Energy Physics, Madison 1980 and Siegen Preprint SI-80-11
10 a) Ch. Gerke: Dissertation, Hamburg (1980), Int. Rep. DESY-PLUTO 80/03 (1980)
10. b) G. Zech: Proceedings of the XIVth Rencontre de Moriond, Vol. 1, p 279 (1979)
10. c) J. L. Siegrist: Ph. D. Thesis SLAC-225, UC-34d (1980)
11. PLUTO Collaboration, Ch. Berger et al.: Z. Phys. C – Particles and Fields **1**, 343 (1979)
12. a) K. Koller, H. Krasemann: Phys. Lett. **88** B, 119 (1979)
12. b) A. Donnachie, P. V. Landshoff: Z. Phys. C – Particles and Fields **4**, 231 (1980)
12. c) T. F. Walsh, P. M. Zerwas: Phys. Lett. **93** B, 53 (1980)
12 d) K. Koller, H. Krasemann: Private communication (1980)
13. R. D. Field, R. P. Feyman: Nucl. Phys. B **136**, 1 (1978)
14. H G. Sander: Private communication
15. T. Sjöstrand: Private communication
16 H. J. Meyer: Dissertation, Siegen (1981)
17 PLUTO Collaboration, Ch. Berger et al.: Phys. Lett. **78** B, 176 (1978)
18. H. Meyer: DESY 79/81 (1979); Proceedings of the 1979 International Symposium on Lepton and Photon Interactions at High Energies, FNAL (1979)
19. Mark II Collaboration, G. S. Abrams et al.: Phys. Rev. Lett. **44**, 114 (1980)
20. PLUTO Collaboration, Ch. Berger et al.: Phys. Lett. **95** B, 313 (1980)
21. LENA Collaboration, P. Bock et al.: Z. Phys. C – Particles and Fields **6**, 125 (1980)